
# Tree-ring based February-April precipitation reconstruction for the lower reaches of the Yangtze River, southeastern China

Jiangfeng Shi, Huayu Lu, Jinbao Li, Shiyuan Shi, Shuangye Wu, Xinyuan Hou, Lingling Li

PII: S0921-8181(15)00091-0
DOI: doi: 10.1016/j.gloplacha.2015.05.006
Reference: GLOBAL 2274

To appear in: *Global and Planetary Change*

Received date: 2 November 2014
Revised date: 5 May 2015
Accepted date: 7 May 2015

Please cite this article as: Shi, Jiangfeng, Lu, Huayu, Li, Jinbao, Shi, Shiyuan, Wu, Shuangye, Hou, Xinyuan, Li, Lingling, Tree-ring based February-April precipitation reconstruction for the lower reaches of the Yangtze River, southeastern China, *Global and Planetary Change* (2015), doi: 10.1016/j.gloplacha.2015.05.006

# Tree-ring based February-April precipitation reconstruction for the lower reaches of the Yangtze River, southeastern China

**Jiangfeng Shi [a, b, *], Huayu Lu [a, b], Jinbao Li [c], Shiyuan Shi [a], Shuangye Wu [a, d], Xinyuan Hou [a], Lingling Li [a]**

[a] *School of Geographic and Oceanographic Sciences, Nanjing University, Nanjing 210023, China*

[b] *Jiangsu Collaborative Innovation Center for Climate Change, Nanjing 210023, China*

[c] *Department of Geography, University of Hong Kong, Pokfulam Road, Hong Kong, China*

[d] *Department of Geology, University of Dayton, Dayton, Ohio, USA*



* Corresponding author at: School of Geographic and Oceanographic Sciences, Nanjing University, Nanjing 210023, China. Tel.: +86 13951608322.
*Email address*: shijf@nju.edu.cn (J. Shi) .

**ABSTRACT**

February-April drought strongly affects agriculture and socio-economics in southeastern China, yet its long-term variability has not been assessed due to the shortness of instrumental records. In this study, we reported a 168-year tree-ring width chronology from a steep, low-elevation site with thin soil layers in the Xianxia Mountains, southeastern China. Contrary to the existing chronologies that are mostly temperature sensitive, this chronology contained a strong February-April precipitation signal, indicating great potential for tree-ring based precipitation reconstructions in southeastern China. The reconstruction explained 47.8% of the instrumental variance during 1951-2012. The full reconstruction indicated that there were 3 dry periods (1873-1896, 1924-1971, 1995-2012) and 2 wet periods (1856-1872, 1972-1994) during 1856-2013. The extreme drought in 2011 was not unprecedented for the past 168 years, and the recent severe droughts may be part of interdecadal variations in regional February-April precipitation. Our results also suggested that February-April precipitation in southeastern China was highly influenced by the tropical Pacific climate system, in particular El Niño-Southern Oscillation (ENSO).

*Keywords:*

*Pinus massoniana*; tree ring; February-April precipitation; ENSO; the Yangtze River; southeastern China

## 1. INTRODUCTION

Southeastern China borders the western Pacific Ocean, and features a typical East Asian monsoon climate (Wang et al., 2005). Spring drought remains a big concern in this populous region. In spring 2011, an extreme drought hit the mid-lower reaches of the Yangtze River with devastating consequences for agriculture and socio-economics of the region (Deng and Luo, 2013). Whether this drought was part of a larger-scale drying trend in recent decades in southeastern China remains unanswered due to the shortness of instrumental records and poor understanding of forcing mechanisms.

The spatio-temporal characteristics of precipitation in southeastern China have been studied during the past two decades, largely based on meteorological data (Zhai et al., 2005; Zou et al., 2005). Annual total precipitation has increased in the lower reaches of the Yangtze River in the second half of the twentieth century (Zhai et al., 2005). Yet the seasonal trends were different, with decreasing spring and autumn precipitation and increasing summer and winter precipitation in southeastern China (Zhai et al., 2005; Deng and Luo, 2013). Due to the decreasing trend and strong interannual variability (Chen et al., 2014), it is critical to study long-term spring precipitation variations in order to fully understand the severity of recent droughts. However, this effort is limited by short instrumental records. Natural proxies, such as tree rings, have the potential to fulfill this task.

Rapid progress in tree-ring studies has been made in East and Southeast Asia in recent years. In Thailand, a soil moisture signal was found in a 448-year teak ring-width chronology (Brendan et al., 2007). March-May Palmer Drought Severity Index (PDSI) series was reconstructed using a 535-year *Fokienia hodginsii* ring-width chronology from northern Vietnam (Sano et al., 2009). A 979-year *Fokienia hodginsii*

ring-width chronology was developed for southern Vietnam, which showed that decades-long droughts in the fourteenth and fifteenth centuries contributed to the demise of Angkor civilization in Cambodia (Buckley et al., 2010). Self-calibrating PDSI was reconstructed using a 1112-year *Pinus sibirica* ring-width chronology from Mongolia, and the reconstruction was used to understand the environmental background for the rise of Mongol Empire and the movement of the empire capital (Pederson et al., 2014). On the Tibetan Plateau, annual precipitation was reconstructed using a 3500-year tree-ring record, and the reconstruction displayed a statistical association with the multidecadal variations of Northern Hemisphere temperatures over the last two millennia (Yang et al., 2014). The 534 grid points of instrumental PDSI were reconstructed with 327 tree-ring chronologies over Monsoon Asia, but only one chronology was from southeastern China (Cook et al., 2010). In general, most of existing precipitation related reconstructions were developed in the arid and semi-arid regions of northern and western China (Shao et al., 2005; Chen et al., 2011; Liu et al., 2011; Bao et al., 2014; Lei et al., 2014). However, in the humid, densely populated southeastern China, most of tree-ring reconstructions were for temperature (Shi et al., 2010; Chen et al., 2012a; Chen et al., 2012b; Duan et al., 2012; Zheng et al., 2012; Duan et al., 2013; Shi et al., 2013). Because annual precipitation is generally larger than 1000 mm, and hot summers experience more precipitation than cold winters in this vast monsoon region, it is common that temperature might be a limiting factor on tree growth rather than precipitation.

Considering the importance of understanding long-term precipitation variations in southeastern China, we made an effort to reconstruct regional precipitation by carefully selecting the tree-ring sampling site. First, to minimize temperature influence, the tree samples should be located at elevations as low as possible. Second,

the sampling site should be on a steep slope with thin soil layer, a condition that soil moisture available to tree growth was limited, especially in dry seasons. In this study, we reported a chronology that was developed from an environment that met the above criteria.

## 2. MATERIAL AND METHODS

### *2.1. Study area and climatic data*

The sampling site is located in the Xianxia Mountains, southwestern Zhejiang province of southeastern China. The Xianxia Mountains extend 100 km from southwest to northeast. They connect the Wuyi Mountains in the southwest and the Yuntai Mountains in the northeast. The average elevation of the Xianxia Mountains is 1000 m above sea level (a.s.l.). The highest mountain is Mt. Jiulong at 1724 m a.s.l., the fourth highest in Zhejiang province. The Xianxia Mountains divide the watershed between the Qiantang River and the Ou River systems.

The climate data used in this study are monthly total precipitation and monthly mean temperature from Quzhou (28º58′N, 118º52′E, 66.9 m a.s.l.), Anqing (30º32′N, 117º3′E, 19.8 m a.s.l.), and Huangshan (30º8′N, 118º9′E, 1840 m a.s.l.) meteorological stations, and monthly total precipitation of ten grids from the global precipitation dataset developed by Climate Research Unit (Mitchell and Jones, 2005) (Fig. 1). The meteorological records were obtained from the China Meteorological Data Sharing Service System. Annual mean temperatures are 17.4 $^{o}$C over the 1951-2013 period at Quzhou station, 16.8 $^{o}$C over the 1951-2013 period at Anqing station, and 8.1 $^{o}$C over the 1956-2013 period at Huangshan station. The corresponding annual total precipitation is 1667.5 mm, 1409.4 mm, and 2333.5 mm (Fig. 2). For all the three stations, peak monthly precipitation is found in June. The

hottest month is July, followed by August and June, while the coldest month is January, followed by February and December. The Southern Oscillation indices (SOI) and Niño3.4 sea surface temperature (SST) data were used for evaluating the effects of the Pacific climte on precipitation change in southeastern China. These data were obtained from the Climate Prediction Center of the National Oceanic and Atmospheric Administration (http://www.cpc.ncep.noaa.gov/data/indices/).

*2.2. Tree-ring data*

The sampling site, named XDC04, is close to the Xiaodai village, Suichang county, southwestern Zhejiang province. It is located at 28º36′N, 119º27′E with an elevation of 380-490 m a.s.l.. It is one of the lowest among more than 40 tree-ring sampling sites that we have collected in the mountains across southeastern China during the past ten years. The slope is north facing and steep (~40º) with thin soil layers. The tree species is *Pinus massoniana*.

Following standard dendrochronological techniques (Cook and Kairiukstis, 1990), two cores per tree were extracted using increment borers. In total, 66 cores from 33 trees were collected. All the samples were processed using standard procedures. They were naturally air dried, mounted on a wooden grove, and sanded gradually until the cells were distinct (Stokes and Smiley, 1996). Then, they were visually cross-dated under microscope. Each tree-ring width was measured to 0.001 mm precision with LINTAB 5.0 system. Dating and measurement errors were further checked with the COFECHA computer program (Holmes, 1983). The original tree-ring width data will be available in the International Tree Ring Databank, www.ncdc.noaa.gov/paleo/treering.html. Subsequently, a ring-width chronology was developed using the ARSTAN program (Cook, 1985) by removing biological growth

trends while preserving variations that were likely related to climate. All the measurement series were detrended by fitting a cubic smoothing spline with a 50% frequency response cutoff equal to 67% of the series length. The ratios between original ring widths and the fitted curves were calculated as the detrended series. The crossdated and detrended series were then merged into a chronology using the biweight robust mean method. As the sample size generally declined in the early portion of a tree-ring chronology, we used the subsample signal strength (SSS) statistic (Wigley et al., 1984) with a threshold of 0.85 to evaluate the most reliable time span of the chronology. In order to preserve more low frequency information, only the tree-ring series extending back before 1900 were kept in the final chronology.

### *2.3. Methods*

The relationships between tree growth and climate were explored by Pearson correlation analysis. The dominant climatic factor on tree growth was reconstructed using a linear regression model. The fidelity of the model was examined by split-sample calibration-verification tests (Meko and Graybill, 1995). The spatial representativeness of the reconstructed precipitation and its connection with global sea surface temperatures (SSTs) were investigated using the KNMI Climate Explorer (http://climexp.knmi.nl). The reconstructed precipitation was compared with two ENSO indices to explore the impact of ENSO on precipitation in southeastern China.

## 3. RESULTS AND DISCUSSION

### *3.1. Tree-ring width chronology*

COFECHA results showed that the mean segment length of the samples was 143

years, with a series intercorrelation of 0.55 and a mean average sensitivity of 0.27. Moreover, the average ring width of all samples was 1.75 mm, and the absent rings accounted for 0.13% of the total rings. The statistics of the standard ring-width chronology (AD 1846-2013) and the results of the common interval analysis (AD 1900-2010) were computed on the detrended data. Relatively large values were obtained for the between-core (R1), within-tree (R2), and between-tree (R3) correlations which were 0.25, 0.43, and 0.25, respectively. The signal-to-noise ratio (SNR) was 14.28, expressed population signal (EPS) was 0.94, and percent variance explained by the first principal component (PC1) was 27.9%. The autocorrelation of the chronology is 0.28. These statistics indicate that the trees showed a common signal likely associated with climate. The final chronology consisted of 54 cores from 31 trees, and covered 1846 to 2013 with the most reliable period from 1856 to 2013 when SSS > 0.85 (Fig. 3).

*3.2. Tree-growth-climate relationship*

Fig. 4 shows the correlation coefficients between the tree-ring chronology and monthly total precipitation and monthly mean temperature during a two-year window. An obvious feature is that precipitation of February and April correlated positively with tree growth at the 0.01 significant level. In contrast, no statistically significant correlation existed with monthly temperature at the 0.01 level. The correlation analysis clearly showed that tree growth at XDC04 was strongly controlled by precipitation in February and April. When the response function analysis was done (Fritts, 1976), we got the same results as the correlation analyses (Fig. 5). February and April were the most significant months. The stress of early growing season moisture on tree growth was also found in other monsoon regions, such as southern

and northern Vietnam and southeastern Tibetan Plateau (Fan et al., 2008; Sano et al., 2009; Buckley et al., 2010; Fang et al., 2010). February temperature at the sampling site is about 6 $^{o}$C (Fig. 2), above which trees are generally thought to begin to grow (Evans et al., 2006; Vaganov et al., 2006; Shi et al., 2008). Therefore, February precipitation has already impacted tree growth. It is noted that the correlation patterns were similar for the two stations further away, (i.e., Anqing and Huangshan), but were slightly different for the Quzhou station. On one hand, the quality of the meteorological records close to the sampling site might not be guaranteed, as shown by validating against records from the surrounding areas. On the other hand, mountain microclimate might have played an important role. At any rate, more tree-ring sampling in this area is needed in order to fully understand the relationship between tree-rings and regional climate.

*3.3. Reconstruction of the February-April precipitation*

Based on the results of the correlation analyses, the February-April total precipitation from the average of the ten CRU grids as shown in Fig. 1 was selected for reconstruction. The calibration model for the early 1951-1980 period showed a correlation coefficient (CC) of 0.702, and the statistics of the CC, reduction of error (RE), and coefficient of efficiency (CE) during the 1981-2012 verification period were 0.711, 0.438, and 0.435 (Table 1). The calibration model using data from the late 1981-2012 period showed a CC value of 0.711, and the CC, RE and CE values during the remaining verification period were 0.702, 0.332, and 0.324. Positive values of RE and CE indicated satisfactory model skill for reconstruction (Cook et al., 1999). The reconstruction accounted for 47.8% of the actual precipitation variance during 1951-2012, which was by far the strongest precipitation signal found in tree-rings in

southeastern China (Fig. 6a). Based on this model, the February-April precipitation was reconstructed with large sample size for the period 1856 to 2013 (Fig. 6b). The reconstructed February-April precipitation will be available on the following web site http://ncde.noaa.gov/paleo.study/18335.

*3.4. Variability of the reconstructed precipitation and its spatial representativeness*

The mean value and standard deviation (SD) of the reconstructed February-April total precipitation for 1856-2013 were 360.0 mm and 54.2 mm, respectively. Extremely wet years were defined with a value above 1.5 SD and an extremely dry year with a value below 1.5 SD. Based on this criteria, 7 extremely dry years and 16 extremely wet years were identified (Table 2). These dry and wet years accounted for 4.4% and 10.1% of the whole period, respectively. An extreme drought occurred in spring 2011 over the mid-lower reaches of the Yangtze River (Deng and Luo, 2013). According to our study, this drought ranked the fifth in the past 168 years, indicating that it was not unprecedented.

On decadal time scales, there were 3 dry periods (1873-1896, 1924-1971, and 1995-2012) and 2 wet periods (1856-1872, and 1972-1994). According to the meteorological records, spring droughts in the 1960s and 2000s and wet episodes in the 1970s-1980s were also found in southern China (Chen et al., 2014), consistent with our study. February-April precipitation showed a decreasing trend at a rate of 9.4 mm per decade at the ten grids during the period 1972-2012 (Figs. 1 & 6a), however, insignificant at the 0.05 level when tested using the method outlined in Wang and Swail (2001). When the trend was put into the context of the past 168 years, it was clear that it may be part of interdecadal variations of February-April precipitation (Fig. 6b). Therefore, the recent decreasing trend should not be overemphasized.

The spatial representativeness of the reconstructed precipitation was explored using KNMI Climate Explorer. The reconstruction could represent February-April precipitation variability over large areas of the lower reaches of the Yangtze River (Figs. 7a-c). The spatial patterns were very similar in the former (1951-1980), latter (1981-2012), or full period (1951-2012), further indicating the temporal stability and reliability of the reconstruction.

*3.5. Teleconnection of the reconstructed precipitation with the Pacific Ocean SSTs*

The reconstructed precipitation correlated negatively with the SSTs in the Western Pacific Warm Pool (WPWP), and positively with that in the east-central equatorial Pacific (Fig. 7d). A consistent pattern was also found using instrumental spring precipitation data in the mid-lower reaches of the Yangtze River (Deng and Luo, 2013). The spring precipitation in the middle and lower reaches of the Yangtze River comes mainly from the western tropical Pacific and partly from the tropical Indian Ocean accompanied by the Western Pacific Subtropical High (WPSH) and the East Asian jet stream moving to the north of their normal position (Zhang et al., 2009). The SST in the western Pacific in winter and spring negatively correlates with the WPSH anomaly (Fan and Liu, 2009). When the WPWP cools, the WPSH strengthens and its position shifts to the west and/or the north that increases spring rainfall in the mid-lower reaches of the Yangtze River (Jiang and Zhao, 2012; Deng and Luo, 2013). We also compared the reconstructed precipitation with the SOI and the Niño3.4 SST series (Fig. 8). The correlation coefficients are -0.34 with the SOI and 0.34 with Niño3.4 SST series over the period 1951-2013, both significant at the 0.01 level. Previous studies showed that El Niño-Southern Oscillation (ENSO) influenced summer precipitation in the mid-lower reaches of the Yangtze River (Chen, 1998).

This study confirmed its impact on February-April precipitation. February-April precipitation in the study region generally increased in an El Niño year, and decreased in a La Niña year.

## 4. CONCLUSIONS

A robust tree-ring width chronology was developed from the Xianxia Mountains, southeastern China. The most reliable interval of the chronology covered the 1856-2013 period. This chronology explained 47.8% of the actual February-April precipitation variance during 1951-2012. The high level of explained variance could be partly attributed to the environment of the sampling site, which was located on a steep, low-elevation slope with thin soils. All these factors led to the high sensitivity of tree rings to February-April precipitation at the sampling site. Our reconstruction revealed three dry periods (1873-1896, 1924-1971, 1995-2012) and two wet periods (1856-1872, 1972-1994) during the past 168 years. It also indicated that the recent severe droughts were merely a manifestation of interdecadal precipitation variability. The drought in February-April 2011 ranked the fifth in the past 168 years, indicating that it was not unprecedented. The reconstructed precipitation was significantly correlated with ENSO, suggesting a strong influence of the tropical Pacific climate on February-April precipitation over the lower reaches of the Yangtze River. Overall, our study indicated great potential of using tree-rings to reconstruct precipitation in humid southeastern China, and to explore the forcings of regional long-term drought variability.

**Acknowledgements**

The authors thank H. Mao, J. Ye, Y. Shi and K. Yu for their help in the field. We are grateful to two anonymous reviewers whose comments helped improve the manuscript. This research was jointly funded by NSFC Project (No. 41271210), the National Basic Research Program of China (973 Program) (No. 2010CB950101), the Fundamental Research Funds for the Central Universities (No. 20620140083), and the Priority Academic Program Development of Jiangsu Higher Education Institutions.

**References**

Bao, G., Liu, Y., Liu, N., Linderholm, H.W., 2014. Drought variability in eastern Mongolian Plateau and its linkages to the large-scale climate forcing. Climate Dynamics, doi:10.1007/s00382-014-2273-7.

Buckley, B.M., Palakit, K., Duangsathaporn, K., Sanguantham, P., Prasomsin, P., 2007. Decadal scale droughts over northwestern Thailand over the past 448 years: links to the tropical Pacific and Indian Ocean sectors. Climate Dynamics 29(1), 63-71.

Buckley, B.M., Anchukaitis, K.J., Peny, D., Fletcher, R., Cook, E.R., Sano, M., Canh Nam, L., Wichienkeeo, A., That Minh, T., Mai Hong, T., 2010. Climate as a contributing factor in the demise of Angkor, Cambodia. Proceedings of the National Academy of Sciences 107(15), 6748-6752.

Chen, F., Yuan, Y., Wei, W., Yu, S., Zhang, T., 2012a. Tree ring-based winter temperature reconstruction for Changting, Fujian, subtropical region of Southeast China, since 1850: Linkages to the Pacific Ocean. Theoretical and Applied Climatology 109, 141-151.

Chen, F., Yuan, Y.J., Wei, W.S., Yu, S.L., Zhang, T.W., 2012b. Reconstructed temperature for Yong'an, Fujian, Southeast China: Linkages to the Pacific Ocean climate variability. Global and Planetary Change 86-87, 11-19.

Chen, J., 1998. The influence of Southern Oscillation in spring and South China Sea High of early summer on summer floods in the middle and lower reaches of the Yangtze River. Quarterly Journal of Applied Meteorology 9(S1), 119-124 (in Chinese with English Abstract).

Chen, S., wu, C., Guo, K., Zhang, X., 2014. A study of the climatic anomaly of the spring precipitation in southern China. Climate Change Research Letters 3,

6-12 (in Chinese with English Abstract).

Chen, Z., He, X., Cook, E.R., He, H.S., Chen, W., Sun, Y., Cui, M., 2011. Detecting dryness and wetness signals from tree-rings in Shenyang, Northeast China. Palaeogeography, Palaeoclimatology, Palaeoecology 302(3-4), 301-310.

Cook, E.R., 1985. A time series analysis approach to tree-ring standardization. Ph.D. Thesis, University of Arizona, Tucson, 171 pp.

Cook, E.R., Kairiukstis, L., 1990. Methods of Dendrochronology: Applications in the Environmental Sciences. Springer, New York, 394 pp.

Cook, E.R., Meko, D.M., Stahle, D.W., Cleaveland, M.K., 1999. Drought reconstructions for the continental United States. Journal of Climate 12(4), 1145-1162.

Cook, E.R., Anchukaitis, K.J., Buckley, B.M., D'Arrigo, R.D., Jacoby, G.C., Wright, W.E., 2010. Asian monsoon failure and megadrought during the last millennium. Science 328(5977), 486-489.

Deng, H., Luo, Y., 2013. Continuous spring and Meiyu rainfall in the mid-lower reaches of the Yangtze during the past 50 years. Journal of Applied Meteorological Science 24(1), 23-31 (in Chinese with English Abstract).

Duan, J., Zhang, Q., Lv, L., 2013. Increased variability in cold-season temperature since the 1930s in subtropical China. Journal of Climate 26(13), 4749-4757.

Duan, J., Zhang, Q.B., Lv, L., Zhang, C., 2012. Regional-scale winter-spring temperature variability and chilling damage dynamics over the past two centuries in southeastern China. Climate Dynamics 39, 919-928.

Evans, M.N., Reichert, B.K., Kaplan, A., Anchukaitis, K.J., Vaganov, E.A., Hughes, M.K., Cane, M.A., 2006. A forward modeling approach to paleoclimatic interpretation of tree-ring data. Journal of Geophysical

Research-Biogeosciences 111, G03008, doi:10.1029/2006JG000166.

Fan, Z.X., Bräuning, A., Cao, K.F., 2008. Tree-ring based drought reconstruction in the central Hengduan Mountains region (China) since AD 1655. International Journal of Climatology 28(14), 1879-1887.

Fan, L., Liu, Q.Y., 2009. Relationship bewteen the Western Pacific Subtropical High and sea-surface temperature anomaly. Journal of Tropical Oceanography 28(5), 83-88 (in Chinese with English Abstract).

Fang, K., Gou, X., Chen, F., Li, J., D'Arrigo, R., Cook, E., Tang, T., Davi, N., 2010. Reconstructed droughts for the southeastern Tibetan Plateau over the past 568 years and its linkages to the Pacific and Atlantic Ocean climate variability. Climate Dynamics 35(4), 577-585.

Fritts, H.C., 1976. Tree Rings and Climate. The Blackburn Press, Caldwell, 567 pp.

Harris, I., Jones, P.D., Osborn, T.J., Lister, D.H., 2014. Updated high-resolution grids of monthly climatic observations – the CRU TS3.10 Dataset. International Journal of Climatology 34(3), 623-642.

Holmes, R., 1983. Computer-assisted quality control in tree-ring dating and measurement. Tree-Ring Bulletin 43(1), 69-78.

Jiang, P., Zhao, P., 2012. The interannual variability of sping rainy belt over southern China and the associated atmospheric circulation anomalies. Acta Meteorologica Sinica 70(4), 681-689.

Lei, Y., Liu, Y., Song, H., Sun, B., 2014. A wetness index derived from tree-rings in the Mt. Yishan area of China since 1755 AD and its agricultural implications. Chinese Science Bulletin 59(27), 3449–3456.

Liu, Y., Wang, C.Y., Hao, W.J., Song, H.M., Cai, Q.F., Tian, H., Sun, B., Linderholm, H.W., 2011. Tree-ring-based annual precipitation reconstruction in Kalaqin,

Inner Mongolia for the last 238 years. Chinese Science Bulletin 56(28), 2995-3002.

Meko, D., Graybill, D.A., 1995. Tree-ring reconstruction of upper Gila River discharge. Water Resources Bulletin 31(4), 605-616.

Mitchell, T.D., Jones, P.D., 2005. An improved method of constructing a database of monthly climate observations and associated high-resolution grids. International Journal of Climatology 25(6), 693-712.

Pederson, N., Hessl, A.E., Baatarbileg, N., Anchukaitis, K.J., Di Cosmo, N., 2014. Pluvials, droughts, the Mongol Empire, and modern Mongolia. Proceedings of the National Academy of Sciences 111(12), 4375-4379.

Rayner, N.A., Parker, D.E., Horton, E.B., Follan, C.K., Alexander, L.V., Rowell, D.P., Ken, E.C., Kaplan, A., 2003. Global analyses of sea surface temperature, sea ice, and night marine air temperature since the late nineteenth century. Journal of Geophysical Research 108(D14), doi: 10.1029/2002jd002670.

Sano, M., Buckley, B.M., Sweda, T., 2009. Tree-ring based hydroclimate reconstruction over northern Vietnam from Fokienia hodginsii: eighteenth century mega-drought and tropical Pacific influence. Climate Dynamics 33(2-3), 331-340.

Shao, X., Huang, L., Liu, H., Liang, E., Fang, X., Wang, L., 2005. Reconstruction of precipitation variation from tree rings in recent 1000 years in Delingha, Qinghai. Science in China (Series D) 48 (7), 939 – 949.

Shi, J., Cook, E.R., Li, J., Lu, H., 2013. Unprecedented January-July warming recorded in a 178-year tree-ring width chronology in the Dabie Mountains, southeastern China. Palaeogeography, Palaeoclimatology, Palaeoecology 381-382, 92-97.

Shi, J., Liu, Y., Vaganov, E.A., Li, J., Cai, Q., 2008. Statistical and process-based modeling analyses of tree growth response to climate in semi-arid area of north central China: A case study of *Pinus tabulaeformis*. Journal of Geophysical Research 113, G01026, doi:10.1029/2007jg000547.

Shi, J.F., Cook, E.R., Lu, H.Y., Li, J.B., Wright, W.E., Li, S.F., 2010. Tree-ring based winter temperature reconstruction for the lower reaches of the Yangtze River in southeast China. Climate Research 41(2), 169-175.

Stokes, M.A., Smiley, T.L., 1996. An introduction to tree-ring dating. The University of Arizona Press, Tucson, 73 pp.

Vaganov, E.A., Hughes, M.K., Shashkin, A.V., 2006. Growth Dynamics of Conifer Tree Rings: Images of Past and Future Environments. Springer, New York, 351 pp.

Wang, P., Clemens, S., Beaufort, L., Braconnot, P., Ganssen, G., Jian, Z., Kershaw, P., Sarnthein, M., 2005. Evolution and variability of the Asian monsoon system: state of the art and outstanding issues. Quaternary Science Reviews 24(5), 595-629.

Wang, X.L., Swail, V.R., 2001. Changes of extreme wave heights in northern hemisphere oceans and related atmospheric circulation regimes. Journal of Climate 14, 2204-2221.

Wigley, T.M.L., Briffa, K.R. and Jones, P.D., 1984. On the average value of correlated time series, with applications in dendroclimatology and hydrometeorology. Journal of Climate and Applied Meteorology 23(2), 201-213.

Yang, B., Qin, C., Wang, J., He, M., Melvin, T.M., Osborn, T.J., Briffa, K.R., 2014. A 3,500-year tree-ring record of annual precipitation on the northeastern Tibetan Plateau. Proceedings of the National Academy of Sciences 111(8), 2903-2908.

Zhai, P.M., Zhang, X.B., Wan, H., Pan, X.H., 2005. Trends in total precipitation and frequency of daily precipitation extremes over China. Journal of Climate 18(7), 1096-1108.

Zhang, J., Zhou, T., Yu, R., Xin, X., 2009. Atmospheric water vapor transport and corresponding anomalous spring rainfall patterns in China. Chinese Journal of Atmospheric Sciences 33(1), 121-134 (in Chinese with English Abstract).

Zheng, Y.H., Zhang, Y., Shao, X.M., Yin, Z.Y., Zhang, J., 2012. Temperature variability inferred from tree-ring widths in the Dabie Mountains of subtropical central China. Trees 26, 1887-1894.

Zou, X.K., Zhai, P.M., Zhang, Q., 2005. Variations in droughts over China: 1951-2003. Geophysical Research Letters 32(4), doi: 10.1029/2004gl021853.

**Figure Captions:**

**Fig. 1.** Map showing the tree-ring sampling site, the meteorological stations, and the ten Climate Research Unit (CRU) grids.

**Fig. 2.** Plot showing the distribution of monthly mean temperature (bar) and monthly total precipitation (square) based on the records from (a) the Quzhou meteorological station (A.D. 1951-2013), (b) Anqing (A.D. 1951-2013), and (c) Huangshan (A.D. 1956-2013).

**Fig. 3.** The tree-ring width standard chronology (solid line) and the corresponding sample size (dashed line).

**Fig. 4.** Correlation coefficients between the tree-ring width chronology and monthly total precipitation (gray bar) and monthly mean temperature (black bar) from previous January to current December at (a) Quzhou (A.D. 1951-2013), (b) Anqing (A.D. 1951-2013), and (c) Huangshan (A.D. 1956-2013) meteorological stations, and (d) a ten-grids averaged regional CRU precipitation dataset (A.D. 1951-2012).

**Fig. 5.** Response function between the tree-ring width standard chronology and monthly total precipitation from a ten-grids averaged regional CRU precipitation dataset (A.D. 1951-2012). * indicates significant at the 0.05 level.

**Fig. 6.** February-April total precipitation reconstruction in the Xianxia Mountains, southeastern China. (a), Comparison of actual (solid line) and reconstructed (dotted line) precipitation for 1951-2012; and (b), the reconstructed precipitation (thin line),

its 10-yr FFT smoothing (thick line) to highlight the low-frequency variability, and the average value (horizontal line) from 1856-2013.

**Fig. 7.** Correlation patterns of the reconstructed precipitation with regional February-April precipitation from CRU TS3.22 (land) over (a) 1951-2012, (b) 1951-1980, and (c) 1981-2012) (Harris et al., 2014), and with (d) concurrent global SSTs from HadISST1 over 1951-2013 (Rayner et al., 2003). Insignificant correlations (i.e. $p > 0.1$) were masked out. The blue circle denotes the sampling site.

**Fig. 8.** Comparison of the reconstructed February-April precipitation with the Pacific climate. (a) The standardized November-April Southern Oscillation Index (SOI) (i.e., difference of the sea level pressure between Tahiti and Darwin, Australia) over 1952-2013, and (b) the Niño3.4 November-April sea surface temperature anomaly over 1951-2013. Note: the right y-axis in Fig. 8(a) was reversed for direct comparison.

**Table 1**

Statistics of calibration and verification test results for the common period of 1951-2012. RE: reduction of error, CE: coefficient of efficiency.

| | Calibration (1951-1980) | Verification (1981-2012) | Calibration (1981-2012) | Verification (1951-1980) | Full calibration (1951-2012) |
|---|---|---|---|---|---|
| r | 0.702 | 0.711 | 0.711 | 0.702 | 0.691 |
| $r^2$ | — | — | — | — | 0.478 |
| RE | — | 0.438 | — | 0.332 | — |
| CE | — | 0.435 | — | 0.324 | — |

**Table 2**

Rank of extremely dry/wet years in the reconstructed February-April precipitation for the lower reaches of the Yangtze River.

| Rank | Dry (mm)/Year | Wet (mm)/Year |
|---|---|---|
| 1 | 226.9/1865 | 508.8/1991 |
| 2 | 245.7/1873 | 491.5/1959 |
| 3 | 251.7/1961 | 484.0/1976 |
| 4 | 259.6/1944 | 469.5/1973 |
| 5 | 268.7/2011 | 468.8/1992 |
| 6 | 271.7/1918 | 464.0/1972 |
| 7 | 275.6/1879 | 462.2/1869 |
| 8 | | 458.9/1975 |
| 9 | | 458.3/1977 |
| 10 | | 457.1/1923 |
| 11 | | 455.5/1950 |
| 12 | | 448.9/2010 |
| 13 | | 448.0/1922 |
| 14 | | 447.4/1983 |
| 15 | | 445.9/2003 |
| 16 | | 443.4/1906 |

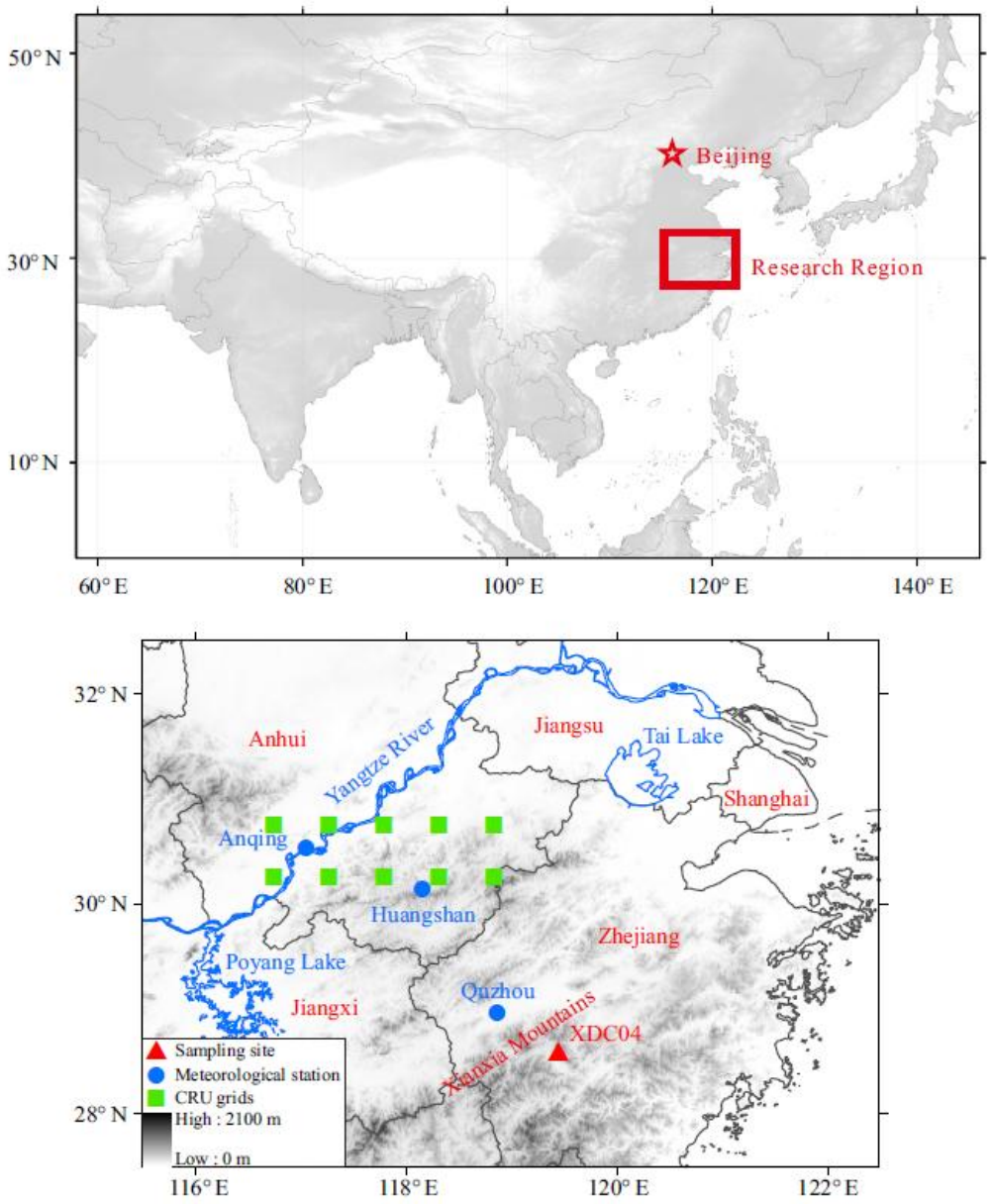


**Figure 1**

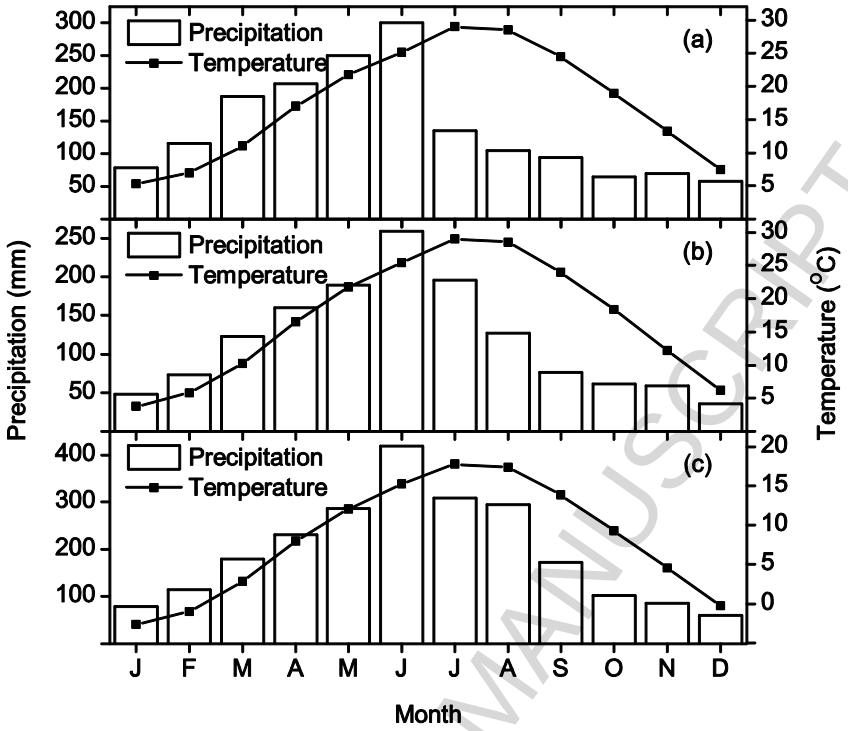


**Figure 2**

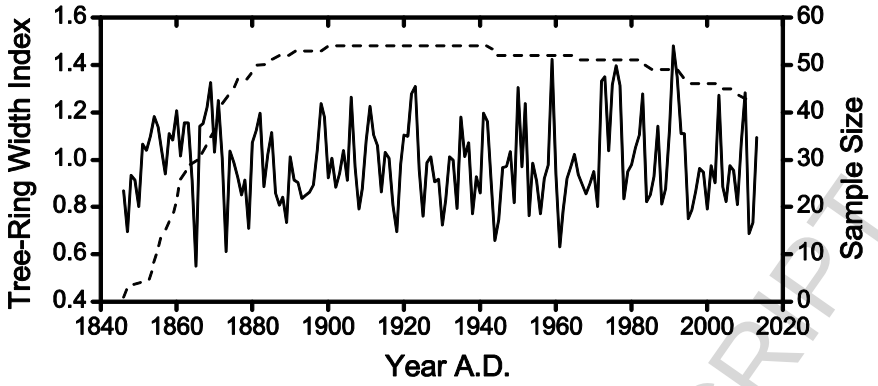


**Figure 3**

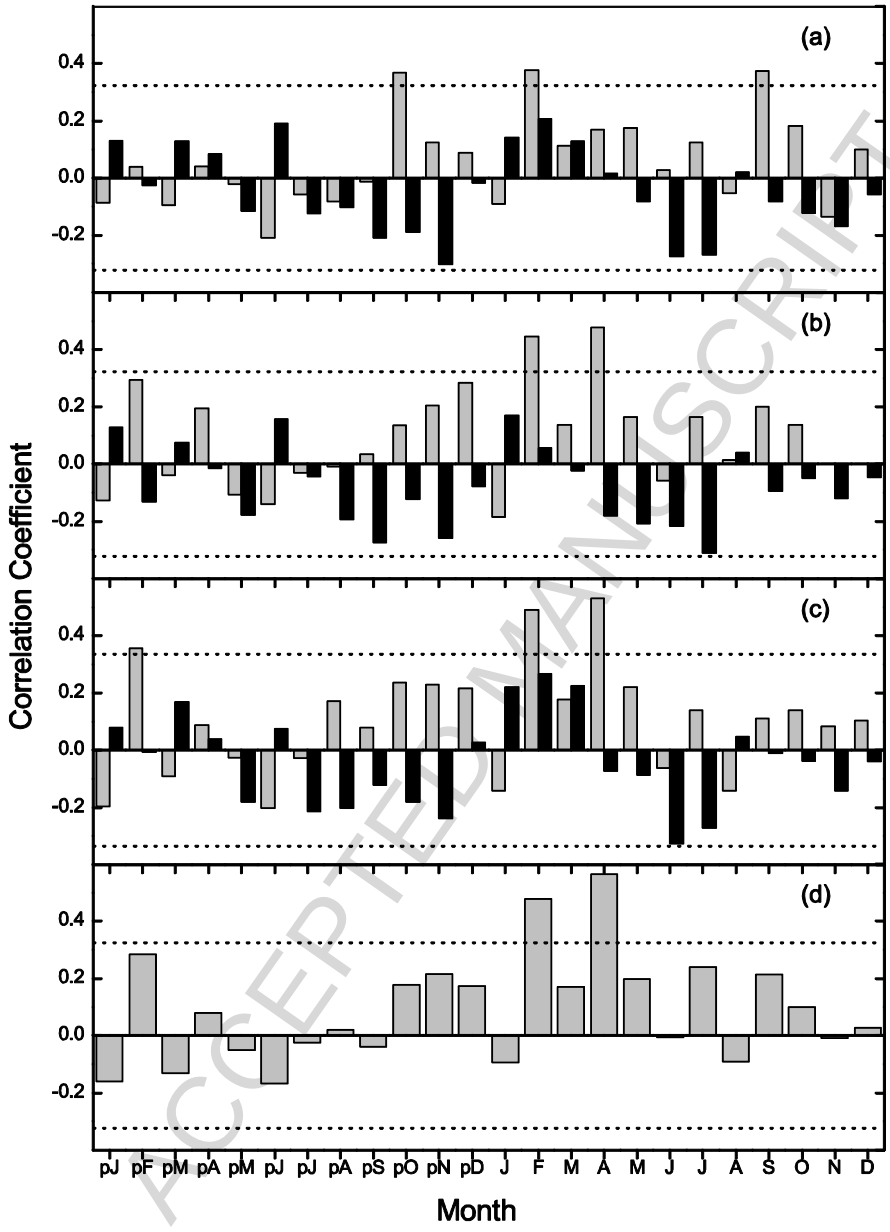


**Figure 4**

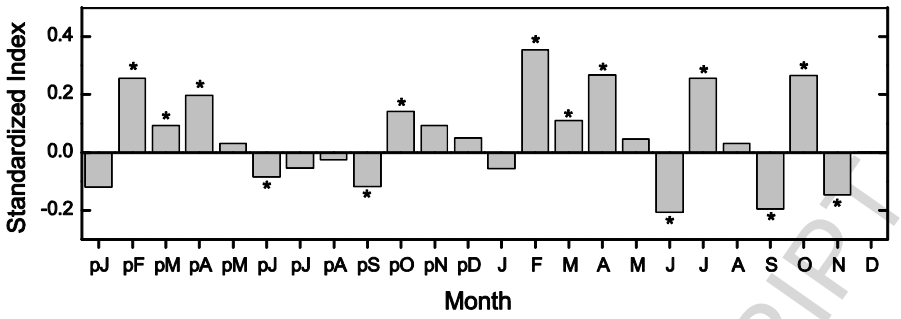


**Figure 5**

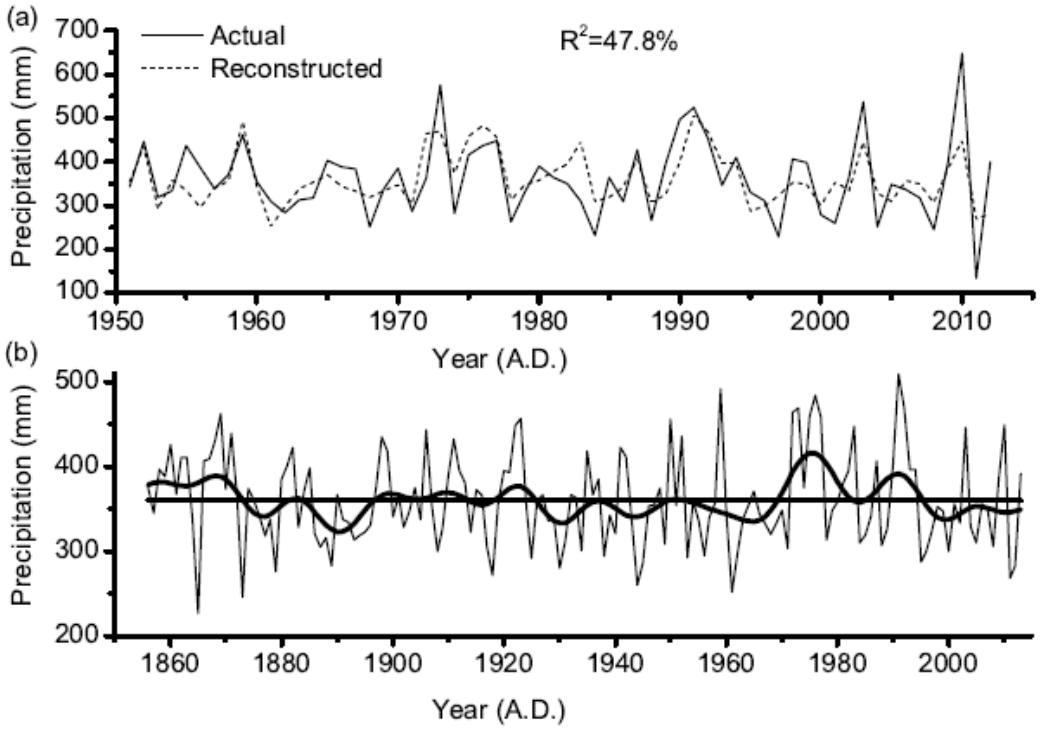


**Figure 6**

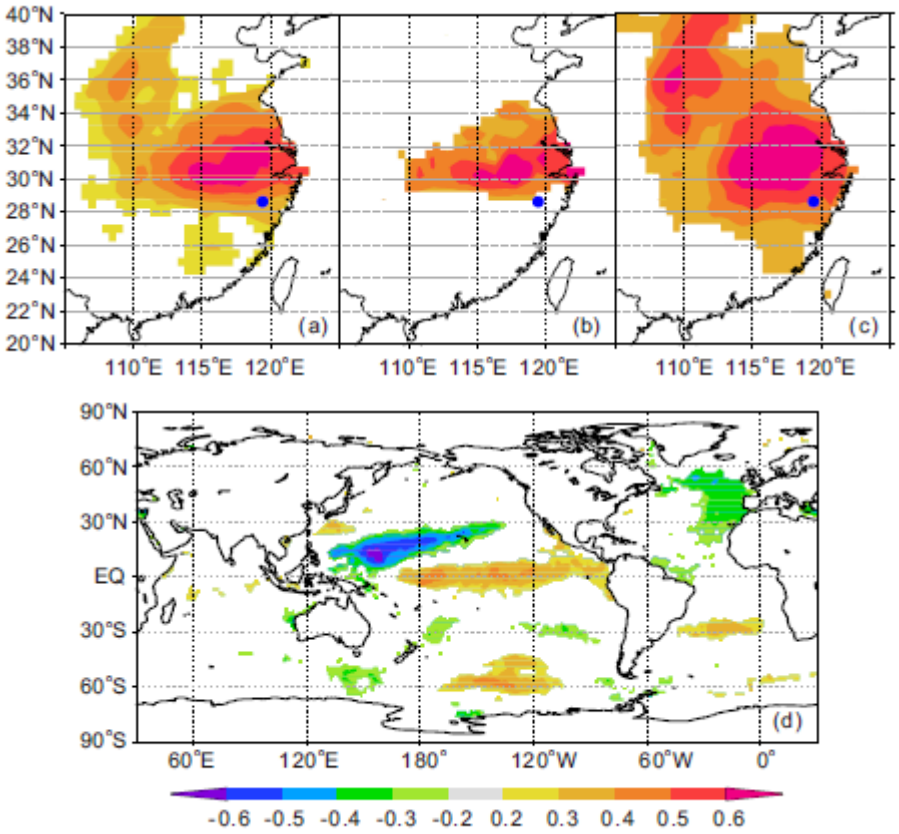


**Figure 7**

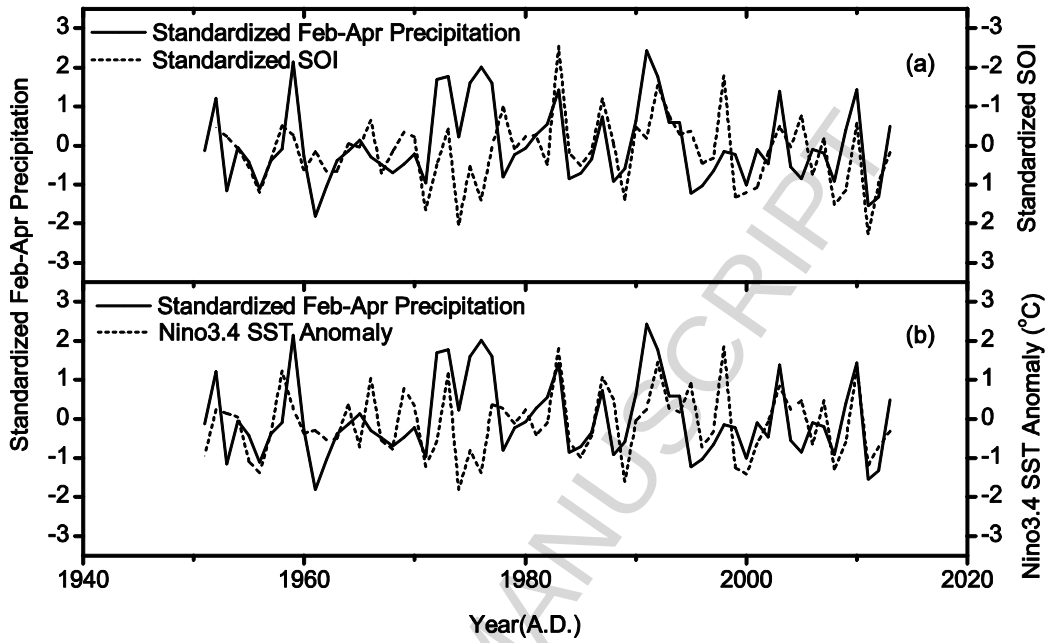


**Figure 8**

**Highlights:**

- We built a tree-ring width chronology in southeastern China.
- We made the first precipitation reconstruction using the chronology.
- The recent observed drought was evaluated in a long-term perspective.
- February-April precipitation was influenced by the tropical Pacific Ocean SST.